HHS Public Access

Author manuscript

Clin Cancer Res. Author manuscript; available in PMC 2018 December 17.

Published in final edited form as:

Clin Cancer Res. 2018 March 15; 24(6): 1415–1425. doi:10.1158/1078-0432.CCR-17-2283.

CD47 Blockade as an Adjuvant Immunotherapy for Resectable Pancreatic Cancer

Alex D. Michaels[1], **Timothy E. Newhook**[1], **Sara J. Adair**[1], **Sho Morioka**[2], **Bernadette J. Goudreau**[1], **Sarbajeet Nagdas**[2], **Matthew G. Mullen**[1], **Jesse B. Persily**[1], **Timothy N. J. Bullock**[3], **Craig L. Slingluff Jr.**[1], **Kodi S. Ravichandran**[2], **J. Thomas Parsons**[2], and **Todd W. Bauer**[1]

[1]Department of Surgery, University of Virginia Health System, Charlottesville, VA 22908

[2]Department of Microbiology, Immunology, and Cancer Biology, University of Virginia Health System, Charlottesville, VA 22908

[3]Department of Pathology, University of Virginia Health System, Charlottesville, VA 22908

Abstract

Purpose: Patients with pancreatic ductal adenocarcinoma (PDAC) who undergo surgical resection and adjuvant chemotherapy have an expected survival of only two years due to disease recurrence, frequently in the liver. We investigated the role of liver macrophages in progression of PDAC micrometastases to identify adjuvant treatment strategies that could prolong survival.

Experimental Design: A murine splenic injection model of hepatic micrometastatic PDAC was used with five patient-derived PDAC tumors. The impact of liver macrophages on tumor growth was assessed by 1) depleting mouse macrophages in nude mice with liposomal clodronate injection, and 2) injecting tumor cells into nude vs. NOD-*scid*-gamma mice.

Immunohistochemistry and flow cytometry were used to measure CD47 (“don’t eat me signal”) expression on tumor cells and characterize macrophages in the tumor microenvironment. *In vitro* engulfment assays and mouse experiments were performed with CD47-blocking antibodies to assess macrophage engulfment of tumor cells, progression of micrometastases in the liver and mouse survival.

Results: *In vivo* clodronate depletion experiments and NOD-*scid*-gamma mouse experiments demonstrated that liver macrophages suppress the progression of PDAC micrometastases. Five patient-derived PDAC cell lines expressed variable levels of CD47. In *in vitro* engulfment assays, CD47-blocking antibodies increased the efficiency of PDAC cell clearance by macrophages in a manner which correlated with CD47 receptor surface density. Treatment of mice with CD47-blocking antibodies resulted in increased time-to-progression of metastatic tumors and prolonged survival.

Corresponding Author: Todd W. Bauer, MD, University of Virginia, Department of Surgery, PO Box 800709, Charlottesville, VA 22908, Phone: 434-924-0391, Fax: 434-982-6552, twb7f@virginia.edu.

Conflicts of Interest: Dr. Bauer has filed provisional patents related to this work, application serial numbers 62/470,432 and 62/470,509. The remaining authors declare no potential conflicts of interest.

Conclusions: These findings suggest that following surgical resection of PDAC, adjuvant immunotherapy with anti-CD47 antibody could lead to substantially improved outcomes for patients.

Keywords

Pancreatic ductal adenocarcinoma; pancreatic cancer; CD47; macrophage; adjuvant therapy

Introduction

Pancreatic cancer is the third leading cause of cancer death in the United States and is projected to be the second by 2020 (1, 2). Surgical resection is the only potentially curative treatment option for pancreatic ductal adenocarcinoma (PDAC); however, even patients who undergo surgery followed by adjuvant chemotherapy have a median survival of only two years due to disease recurrence (3). As most of these recurrences are in the liver, patients likely harbor occult hepatic micrometastases at the time of surgery (4–7). The survival, growth, and eventual progression of these micrometastases are heavily influenced by the interactions between the cancer cells and the immune system (6, 8). As part of the reticuloendothelial system, the liver has large populations of both resident liver macrophages (RLMs) and infiltrating macrophages (9, 10). Given the propensity of PDAC to metastasize to the liver via the hepatic portal system, we sought to investigate the role of macrophages in the progression of PDAC micrometastases in order to identify adjuvant treatment strategies that could increase the chances of cure.

Macrophages associated with primary tumors have been shown to have predominantly pro-tumor and immunosuppressive effects in many cancer types and are known to be associated with a worse prognosis in PDAC (11, 12). However, in metastatic disease, there is less of a consensus about the role of metastasis-associated macrophages (MAMs), with studies demonstrating both pro-tumor and anti-tumor activity in various cancers (13–18). Though macrophages can mediate their anti-tumor activity through a variety of mechanisms, Gül *et al.* showed that phagocytosis is the major way that liver macrophages clear tumor cells (18). In order to evade phagocytosis by macrophages, many cancers including PDAC express high levels of CD47, a transmembrane protein that acts as an anti-phagocytic “don’t eat me” signal (19–23). We hypothesized that CD47 expression may allow PDAC micrometastases to escape elimination by the innate immune system, and therefore might be a good target for adjuvant pancreatic cancer therapy.

In this work, we used a validated model of hepatic micrometastatic PDAC to characterize the interactions between the innate immune system and PDAC micrometastases. This model focuses on previously established portal-vein derived micrometastases, recapitulating the clinical post-resection state in patients with occult hepatic micrometastases without a primary tumor present. We first demonstrated that liver macrophages suppress the progression of PDAC micrometastases. We observed that the surface receptor density of CD47 varies widely among patient-derived PDAC cell lines, that *in vitro* CD47 blockade can enhance the ability of macrophages to engulf tumor cells, and that the magnitude of this effect could be predicted by CD47 receptor density levels. Finally, we found that treatment

with an anti-CD47 antibody can protect against PDAC micrometastases with decreased hepatic tumor burden, increased time-to-progression, and prolonged survival in an *in vivo* model.

Materials and Methods

Derivation of Patient-Derived Cell Lines and Lentiviral Transduction

PDAC tumor samples MAD 09-366, 12-395, 14-449, 08-608, 08-738 (T366, T395, T449, T608, and T738, respectively) were generated from remnant human tumor surgical pathology specimens collected in collaboration with the University of Virginia Biorepository and Tissue Research Facility and with the approval of the University of Virginia Institutional Review Board for Health Sciences Research following written informed consent from each patient. Tumors were propagated orthotopically on the pancreata of immunocompromised mice and cell lines were established, as previously described (24, 25). Cells were transduced with firefly luciferase lentivirus (KeraFAST, Boston, MA) and maintained as previously described (26). Fresh cell aliquots were thawed, propagated, and used for experiments every four months.

Adjuvant Murine Model of Hepatic Micrometastatic PDAC with In Vivo Bioluminescence Imaging

Six- to eight-week old male athymic nude (Foxn1^{nu}) mice (Envigo, Indianapolis, IN) or NOD *scid* gamma (NOD.*Cg-Prkdc*^{scid} *Il2rg*^{tm1Wjl}/SzJ) mice (The Jackson Laboratory, Bar Harbor, ME) were used for all *in vivo* experiments. As previously described, one million luciferase-expressing, patient-derived PDAC cells were injected into the spleen, the cells were allowed to circulate for ten minutes, then a splenectomy was performed, and the abdomen was closed (26). Following splenic injection of PDAC cells, hepatic tumor burden was followed by serial *in vivo* bioluminescence imaging. Figure 1A shows a schematic of PDAC cell line establishment and this *in vivo* model. Luminescence was captured with an IVIS Spectrum in vivo imaging system (PerkinElmer, Waltham, MA) and quantified as surface radiance (photons/sec/cm^2/steradian) using Living Image software, version 2.50 (Caliper Life Sciences, Hopkinton, MA), as previously described (26). Data are expressed as hepatic tumor burden relative to 48 hours post-injection for all *in vivo* experiments, except the delayed-treatment experiment in which case tumor burden at 15 days post-injection was used as the baseline. Time-to-progression (TTP) is defined as the number of days post-injection until relative hepatic tumor burden reaches 2.0. Overall survival (OS) is defined as the number of days post-injection until predefined endpoints requiring euthanasia have been met such as >20% weight loss, extreme lethargy, decreased mobility, tumor size >2 cm, or moribund status. This research was conducted with the approval of the University of Virginia Animal Care and Use Committee.

Histologic Evaluations

Sections of murine livers following splenic injection of PDAC cells were collected at necropsy then paraffin-embedded and stained with hematoxylin and eosin (H&E) by the University of Virginia Research Histology Core using standard methods. IHC staining was performed by the Biorepository and Tissue Research Facility with an anti-F4/80 antibody

(Bio-Rad Laboratories, Hercules, CA). Images were obtained using an Aperio ScanScope slide scanner or a Leica DMRBE microscope, Leica DFC420 camera, and Leica FireCam software, version 3.1 (Leica Microsystems, Wetzlar, Germany).

Hepatic Macrophage Depletion

Mice were treated with anionic clodronate liposomes (56 mg/kg intraperitoneal [i.p.]) (FormuMax, Palo Alto, CA) 48 hours prior to splenic injection of PDAC cells then on post-splenic injection days 3, 8, 12, and 19 to selectively deplete liver macrophages (27).

Flow Cytometry

Following *in vivo* macrophage depletion experiments, murine livers were minced and digested using 150 units/ml of collagenase type I (Worthington Biochemical, Lakewood, NJ) in Iscove's Modified Dulbecco's Medium (Life Technologies, Grand Island, NY) for three hours, rotating at 37°C. Dissociated cells were then passed over a 70 μm filter and treated with red blood cell lysis buffer (Miltenyi Biotec, Bergisch Gladbach, Germany). Cells were then stained with LIVE/DEAD fixable yellow stain (Thermo Fisher Scientific, Waltham, MA) and fixed with 2% paraformaldehyde. Cells were stained with antibodies against F4/80 (Bio-Rad Laboratories, Hercules, CA) and CD11b (BioLegend, San Diego, CA). After exclusion of dead cells, resident liver macrophages were defined as $F4/80^{high}CD11b^{low}$ cells and circulating monocytes were defined as $F4/80^{low}CD11b^{high}$ cells.

For flow cytometry performed on cultured PDAC cell lines, cells were harvested and passed over a 70 μm filter. Fc receptor blocking reagent (Miltenyi Biotec, Bergisch Gladbach, Germany) was used per the manufacturer's instructions. Cells were then stained with antibodies against epithelial cell adhesion molecule (EpCAM) and CD47 (Miltenyi Biotec, Bergisch Gladbach, Germany) followed by 4',6-diamidino-2-phenylindole (DAPI) viability dye (Roche Diagnostics, Indianapolis, IN). After exclusion of dead cells, PDAC cells were identified as $EpCAM^{+}$. PDAC cell lines were then characterized by CD47 median fluorescence intensity (MFI) and median forward scatter height (FSC), which is proportional to cell diameter. CD47 receptor density index (RDI), or the relative number of CD47 molecules per unit membrane area, is defined as $MFI/FSC^2 \times 10^8$ and is expressed in arbitrary units.

The above experiments were all performed in the University of Virginia Flow Cytometry Core Facility using a FACSCalibur flow cytometer (BD Biosciences, San Jose, CA) and analyzed using FlowJo software, version 9.8.2 (FlowJo, Ashland, OR).

Antibodies

The B6H12.2 mouse anti-human CD47 hybridoma was obtained from ATCC (Manassas, VA). The cells were cultured and the antibody (αCD47) was purified by the University of Virginia Antibody Engineering and Technology Core. Purified IgG from mouse serum (mouse IgG) was obtained from Protein Mods (Madison, WI).

Macrophage Isolation and In Vitro Engulfment Assay

Peritoneal macrophages were obtained as previously described (28). In brief, the peritoneal cavity of a C57BL/6 mouse was flushed with phosphate-buffered saline (PBS) containing 10% fetal bovine serum. Collected cells were then spun down and resuspended in X-VIVO 10 serum-free hematopoietic cell medium (Lonza Group, Basel, Switzerland). Macrophages were plated in a 24-well plate (10^5 cells/well) for use two days later.

Macrophages were stained with carboxyfluorescein succinimidyl ester (CFSE) (Tonbo Biosciences, San Diego, CA). PDAC cells were harvested and stained with CypHer5E (GE Healthcare, Chicago, Illinois), a pH-sensitive dye which fluoresces red in acidic conditions such as a lysosome, and then treated with either mouse IgG or αCD47 (50 μg/ml) at 4°C for 30 minutes. PDAC cells were then added to the macrophages at a ratio of 5:1 and incubated together at 37°C for four hours. Non-engulfed PDAC cells were then washed off three times with PBS, macrophages were dissociated from the plate with trypsin, and engulfment was assessed by flow cytometry. Cells were analyzed with a FACSCanto I flow cytometer (BD Biosciences, San Jose, CA) FlowJo software, version 9.8.2 (FlowJo, Ashland, OR). Non-phagocytic macrophages were identified as being $CFSE^+$ only, whereas phagocytic macrophages were identified as being both $CFSE^+$ and $CypHer5E^{high}$. Figure 3A shows a schematic of the engulfment assay protocol. Percent Engulfment was defined as: $\frac{\#\ \text{Phagocytic Macrophages}}{\#\ \text{Phagocytic Macrophages} + \#\ \text{Non} - \text{Phagocytic Macrophages}} \times 100$. Δ Engulfment was defined as: $\frac{\text{Percent Engulfment}_{\alpha\text{CD47} - \text{Treated}}}{\text{Percent Engulfment}_{\text{Mouse IgG} - \text{Treated}}}$.

In Vivo Antibody Treatment

Forty-eight hours after splenic injection of PDAC cells, baseline hepatic tumor burden was assessed with bioluminescence imaging. Mice were then treated with either αCD47 (200 μg/day i.p.), mouse IgG (200 μg/day i.p.), or no therapy. Hepatic tumor burden was assessed at regular intervals and TTP and OS were determined, as above.

Statistical Analysis

Either Mann-Whitney test or Kruskal-Wallis test with Dunn's test for multiple comparisons were used to compare tumor burdens. Two-way ANOVA with repeated measures was used to compare growth curves under different treatments. Paired t-test was used to compare engulfment percentages under different treatments. The correlation between CD47 RDI and Δ Engulfment was analyzed using Pearson's correlation. TTP and OS among treatment groups were compared using log-rank test. All tests were two-sided with a threshold p value for significance of 0.05. Prism software, version 7.00 (GraphPad Software, La Jolla, CA) was used for all statistical analyses.

Sample sizes were based on our experiences with the murine splenic injection model of adjuvant micrometastatic PDAC that six biologic replicates are sufficient to identify statistically significant differences in tumor burden and survival among treatment groups. Biologic replicates were excluded if the mouse died as a result of the initial surgery (within one week postoperatively) or if the mouse had no clearance of tumor burden as this very rare

finding (three mice total in these studies) is often associated with surgery-related morbidity. As the surgical procedure takes about 30 minutes per cage of four mice, cages were not randomized to treatment groups; instead, an equal number of cages from early, middle, and late surgical times during the operative day were allocated to each treatment group to minimize the effects of surgical timing. Blinding was not performed as some experiments compared visibly different strains of mice and others involved treatment and measurement performed simultaneously. All endpoints were prospectively selected.

Results

Hepatic Healing and Tumor Clearance Occur Early Following Splenic Injection of PDAC Cells

Twenty-four hours after the splenic injection of T608 PDAC cells (Figure 1A), cancer cells were observed within and surrounding hepatic portal veins with corresponding areas of regional hepatic ischemic injury and decreased cellularity (Figure 1B). There was rapid remodeling of hepatic parenchyma with a decrease in hepatic injury from 11.9% of tissue area at 24 hours to 7.6% at 48 hours. By 22 days, there were small foci of metastases in the liver, with progressive liver replacement over time. Serial *in vivo* bioluminescence imaging reveals a phase of early tumor clearance, followed by a variable dormancy period (marked by no net increase in tumor cells), and eventually proliferative outgrowth (Figure 1C). Each PDAC cell line demonstrated unique, reproducible growth kinetics (Figure 1D).

Liver Macrophages Suppress the Progression of PDAC Micrometastases

The prior splenic injections were performed in athymic nude mice, which lack a functional cell-mediated immunity but have a functional innate immunity, enabling a specific assessment of the role of the innate immune system. As we observed concomitant healing of tissue injury and clearance of tumor cells in an immunologic organ, we hypothesized a role of the innate immune system in these processes. To test whether innate immune effectors may contribute to transient tumor dormancy, two PDAC cell lines were injected in matched cohorts of both nude mice and NOD *scid* gamma (NSG) mice (which lack cell-mediated immunity as well as functional macrophages, dendritic cells, natural killer (NK) cells, and cytokine signaling). NSG mice had significantly less tumor clearance by seven days than nude mice for both T608 (55% vs 88%, p=0.003) and T366 (48% vs 81%, p=0.02), as shown in Figure 2A and 2B. Additionally, NSG mice had significantly reduced time-to-progression (TTP) of tumors compared with nude mice for both T608 (median 21 d vs 35 d, p<0.001) and T366 (median 28 d vs NR, p<0.001), as shown in Figure 2C and 2D.

Given the large population of macrophages in the liver and the emerging literature about the role of MAMs in metastatic progression, we hypothesized that macrophages have a role in the clearance PDAC cells. To assess this, tumor burden of T608 was compared in nude mice treated with clodronate to deplete RLMs vs. control-treated mice. Macrophage-depleted mice had significantly increased hepatic tumor burden through twenty-six days (p<0.001) (Figure 2E). Immunohistochemistry (IHC) for F4/80 demonstrated an abundance of hepatic macrophages surrounding PDAC cells in the untreated mice (Figure 2F, top) while this response was absent in clodronate-treated mice (Figure 2F, bottom). Flow cytometric

analysis of liver digests demonstrated that administration of liposomal clodronate selectively depleted RLMs (Figure 2G and Supplementary Figure S1).

CD47 Receptor Density Varies Among Patient-Derived PDAC Cell Lines

We hypothesized that the ability of macrophages to control PDAC micrometastases may be enhanced by blocking CD47. Previous studies have shown that upon binding of CD47 expressed on a target cell (cancer cell) to signal-regulatory protein alpha (SIRPα) on a macrophage, a dephosphorylation cascade is initiated which results in the inhibition of myosin accumulation at the macrophage surface, thereby blocking phagocytosis (29). The CD47 surface expression of five patient-derived PDAC cell lines was characterized using flow cytometry (Table 1). The anti-phagocytic effects of CD47 are mediated locally at the phagocytic synapse and are dependent on CD47 expression at the site of macrophage binding (29). We therefore also calculated the CD47 receptor density index (RDI), or the relative number of CD47 molecules per unit membrane area, for each cell line. CD47 RDI ranged from 3.5 to 12.9 arbitrary units (AU) which allowed for the examination of the efficacy of CD47 blockade as a function of CD47 RDI.

CD47 Blockade Enhances the Engulfment of Patient-Derived PDAC Cells

Given that macrophages play an important role in clearing metastatic PDAC (Figure 2) and that we detected CD47 expression in primary PDAC cells (Table 1), we hypothesized that macrophages can engulf PDAC cells, and that blocking CD47 on PDAC cells could increase the efficiency of tumor cell clearance by macrophages. To test these hypotheses, we performed an *in vitro* engulfment assay (Figure 3A). First, we found that macrophages are able to engulf primary PDAC cells. Treatment with an anti-CD47 blocking antibody (αCD47) had negligible effects on the engulfment of the two PDAC cell lines with the lowest levels of CD47 RDI, but did significantly increase engulfment of the three cell lines with the highest CD47 RDI (Figure 3B). Importantly, there was a strong positive correlation (R^2=0.94) between CD47 RDI and the *in vitro* efficacy of αCD47 to enhance engulfment (Figure 3C). This suggests that blocking CD47 facilitates the removal of PDAC cells via macrophage-dependent phagocytosis, and that PDAC cells with high levels of CD47 are especially susceptible to treatment.

CD47 Blockade Decreases Metastatic PDAC Tumor Burden and Improves Outcomes

We investigated whether the above-described *in vitro* results would translate *in vivo* using an adjuvant model of hepatic micrometastatic PDAC. Splenic injections of the patient-derived PDAC cell lines with the highest, median, and lowest levels of CD47 RDI were performed. Mice were treated with daily αCD47, mouse IgG, or no treatment. Within two days of initiating therapy, tumor burden was decreased in mice bearing T608 (the PDAC cell line with the highest CD47 RDI) treated with αCD47 compared to mice receiving mouse IgG or no therapy (0.19 vs 0.44 vs 0.69, p=0.005 for αCD47 vs mouse IgG and αCD47 vs no treatment). By three weeks, there was continued efficacy of αCD47 in mice bearing T608 (Figure 4A), whereas there were no differences in tumor burden seen in mice bearing T366 which has the lowest CD47 RDI (Figure 4C). αCD47 had intermediate efficacy in mice bearing T395 which has the median CD47 RDI (Figure 4B). Given the lack of effect of αCD47 in T366, we stopped treating mice bearing T366 after three weeks of treatment and

continued treating mice bearing T608 and T395 for seven weeks total. Ten weeks post-splenic injection of PDAC cells, T608 mice treated with αCD47 exhibited significantly less tumor burden than either of the control treatment groups (Figure 4D). αCD47 also showed an effect in T395 mice (Figure 4E), whereas no differences were seen in T366 mice (Figure 4F). Follow-up T608 splenic injection experiments showed a similar efficacy of a three-week αCD47 treatment course compared to the seven-week course (Figure 5A) and that there is inhibition of tumor growth even if the onset of αCD47 treatment is delayed to post-injection day 15 (Figure 5B).

These results translated into significantly prolonged TTP for T608 αCD47-treated mice compared to those mice that received mouse IgG or no therapy (no treatment vs IgG: p=0.12, no treatment vs αCD47: p<0.0001, IgG vs αCD47: p=0.002) (Figure 4G). αCD47 again showed intermediate efficacy in mice bearing T395 (no treatment vs IgG: p=0.008, no treatment vs αCD47: p=0.002, IgG vs αCD47: p=0.83) (Figure 4H) and no efficacy in T366 (Figure 4I). Similar trends held for overall survival with αCD47 treatment showing the greatest effect in T608 mice (no treatment vs IgG: p=0.04, no treatment vs αCD47: p=0.002, IgG vs αCD47: p=0.26) (Figure 4J), a modest effect in T395 mice (no treatment vs IgG: p=0.006, no treatment vs αCD47: p=0.002, IgG vs αCD47: p=0.86) (Figure 4K), and no effect in T366 mice (Figure 4L).

Discussion

The goal of adjuvant therapy is to target any residual cancer cells to prevent the eventual development of overt metastases and, thus, improve survival (30). Despite successful surgical resection and current standard-of-care adjuvant chemotherapy, patients with localized pancreatic cancer have an expected survival of only two years, often due to the progression of micrometastatic disease in the liver. We therefore conducted preclinical *in vitro* and *in vivo* experiments investigating the interactions between PDAC and the innate immune system in the micrometastatic niche of the liver. Using a murine model of hepatic micrometastatic PDAC with patient-derived cell lines, we identified a tumor-suppressing role for liver macrophages. We demonstrated that *in vitro* CD47 blockade can increase the engulfment of PDAC cells by macrophages, and that *in vivo* treatment with an anti-CD47 antibody can enhance the natural ability of liver macrophages to protect against PDAC micrometastases.

In these experiments, we found that RLMs suppress the progression of PDAC micrometastases in the liver. Griesmann *et al.* found that depletion of RLMs in the KPC (*Kras*^{G12D};*Trp53*^{R172H};*Pdx1-Cre* mice) genetically engineered mouse model of PDAC led to a reduction in the number of metastases (31). Similarly, it has been shown that cytokines released from RLMs enhance the binding of colon cancer cells to the endothelium, a critical step in metastasis (14). Though both of these studies suggest a pro-tumor role for macrophages, they were investigating the formation of metastases through the processes of cancer cell extravasation and liver seeding. In contrast, our splenic injection model of PDAC specifically evaluates the progression from established micrometastases to clinically detectable recurrences. Studies in similar models of colon cancer and melanoma portal vein-derived metastasis to the liver have shown that RLMs phagocytose tumor cells and that their

ablation leads to the progression of metastases (13, 15, 18). Nielsen *et al.* showed that the population of pro-tumoral MAMs comprises infiltrating macrophages, not RLMs (16). By treating with liposomal clodronate, we ablated RLMs while preserving infiltrating macrophages and accordingly observed accelerated tumor progression.

The observed suppressive role of RLMs on PDAC micrometastases in the liver prompted an investigation into the effects of anti-CD47 therapy on disease progression. We confirmed the findings of prior studies that CD47 expression is elevated on multiple cancers, including PDAC, and that CD47 blockade leads to increased engulfment of cancer cells by macrophages *in vitro* (19, 22, 32). Though there are additional “eat me” and “don’t eat me” signals that together determine baseline levels of cancer cell engulfment, we identified CD47 RDI as a strong predictor of the magnitude of increased *in vitro* engulfment with anti-CD47 treatment (33)0. Importantly, we observed a similar correlation between CD47 RDI and the *in vivo* efficacy of αCD47 antibody to decrease metastatic tumor burden, increase TTP, and prolong survival in our model. This could allow for the development of CD47 RDI as a clinical biomarker for identifying patients most likely to benefit from αCD47 therapy. This could have immediate applicability in the ongoing clinical trials (clinicaltrials.gov) of anti-CD47 therapy for patients with hematologic malignancies or advanced solid tumors.

The current understanding of the role of CD47 in the progression of pancreatic malignancies is limited to events and interactions occurring at the primary tumor site. Krampitz *et al.* showed that anti-CD47 therapy inhibits tumor growth and prevents metastasis in an orthotopic model of pancreatic neuroendocrine tumors (34). Cioffi *et al.* reported significant slowing of subcutaneous PDAC xenografts with a combination of chemotherapy plus αCD47 but no growth inhibition with either chemotherapy alone or αCD47 alone (19). Consistent with the parallel progression model, metastasis is an early event in the natural history of pancreatic cancer and metastatic tumors are biologically different from their primary progenitor tumors (35–39). As such, we aimed to describe the effects of CD47 blockade specifically in the micrometastatic environment. Despite administering only 40% of the daily dose of αCD47 that Cioffi *et al.* described, we observed *in vivo* efficacy of αCD47 monotherapy in our adjuvant model. These findings can be explained by the unique features of the hepatic micrometastatic niche. The liver harbors the majority of the body’s macrophages, and unlike the subcutaneous tissues which have relatively low levels of blood flow, the liver receives 25% of cardiac output while accounting for only 2.5% of body weight, which allows for efficient delivery of drug to the tumor (10, 40). Further, there are far fewer tumor cells in micrometastases than in a bulky primary tumor. Together this leads to a drug-rich environment with a high ratio of effector cells to target cells. As Cioffi *et al.* showed additive effects of αCD47 therapy and chemotherapy, we would anticipate similar synergy in the micrometastatic setting leading to substantial improvements in clinical outcomes. At the time of surgical resection, micrometastatic tumor burden in patients with PDAC has been present for an indeterminate amount of time. As αCD47 therapy was effective both soon after PDAC cell introduction to the liver and as a delayed treatment, our findings suggest a wide window of therapeutic opportunity.

Because we used patient-derived cancer cells in the present studies, all *in vivo* experiments were performed with immunocompromised mice. Though athymic nude mice are ideal for

investigating the interactions between the innate immune system and human cancer cells, we are unable to assess effects of the acquired immune system in our model (41). The priming of an anti-tumor T-cell response following CD47-mediated engulfment of cancer cells has been described, which could contribute to improved long-term latency (23). Therefore, our model potentially underestimates the overall efficacy of αCD47. Similarly, athymic nude mice lack a functional cell-mediated immunity resulting in decreased opsonization. While CD47 is considered a "don't eat me" signal, opsonization by IgG is an "eat me" signal (42). To account for this effect, we chose to use both purified IgG from mouse serum and no treatment instead of an isotype control in our experiments. This can account for the decreased tumor burden and prolonged TTP for mice bearing T608 and T395 which received mouse IgG treatment compared to mice who received no treatment. This fact also makes the differences in αCD47- vs mouse IgG-treated mice even more meaningful. Therefore, we posit that anti-CD47 therapy will be more effective in immunocompetent individuals. Our group developed a syngeneic splenic injection model of hepatic micrometastatic PDAC using KPC-derived tumors in order to investigate the interplay between the innate and acquired immune systems in fully immunocompetent mice. Unfortunately, these KPC cell lines have proven to be too aggressive to allow for the reliable detection of changes in metastatic growth kinetics and progression under different experimental conditions. To overcome this obstacle, we are pursuing using our patient-derived cell lines in a humanized mouse model which should most accurately recapitulate disease progression in our patient population.

Current adjuvant treatment following surgical resection of PDAC is suboptimal. Collectively, our findings suggest that post-resection CD47 blockade could lead to substantial improvements in patient outcomes. Therefore, these data support a clinical trial of CD47 blockade as an adjuvant immunotherapy for pancreatic cancer.

Supplementary Material

Refer to Web version on PubMed Central for supplementary material.

Acknowledgements

The authors thank Laurie Edwards for her assistance with experiments and animal care. The authors also thank Anita Impagliazzo for illustrating the schematic in Figure 1A. **Financial Support:** NIH T32 AI007496 (ADM), NIH T32 CA163177 (TEN, MGM), NIH T32 CA009109 (SN), the UVA Cancer Center through the NCI Cancer Center Support Grant P30 CA44579, and support from the Commonwealth of Virginia.

References

1. Siegel RL, Miller KD, Jemal A. Cancer Statistics, 2017. CA Cancer J Clin. 2017;67:7–30. [PubMed: 28055103]
2. Rahib L, Smith BD, Aizenberg R, Rosenzweig AB, Fleshman JM, Matrisian LM. Projecting cancer incidence and deaths to 2030: the unexpected burden of thyroid, liver, and pancreas cancers in the United States. Cancer Res. 2014;74:2913–21. [PubMed: 24840647]
3. Neoptolemos JP, Palmer DH, Ghaneh P, Psarelli EE, Valle JW, Halloran CM, et al. Comparison of adjuvant gemcitabine and capecitabine with gemcitabine monotherapy in patients with resected pancreatic cancer (ESPAC-4): a multicentre, open-label, randomised, phase 3 trial. Lancet. 2017;389:1011–24. [PubMed: 28129987]

4. Griffin JF, Smalley SR, Jewell W, Paradelo JC, Reymond RD, Hassanein RE, et al. Patterns of failure after curative resection of pancreatic carcinoma. Cancer. 1990;66:56–61. [PubMed: 2354408]
5. Sperti C, Pasquali C, Piccoli A, Pedrazzoli S. Recurrence after resection for ductal adenocarcinoma of the pancreas. World J Surg. 1997;21:195–200. [PubMed: 8995078]
6. Fidler IJ, Kripke ML. The challenge of targeting metastasis. Cancer Metastasis Rev. 2015;34:635–41. [PubMed: 26328524]
7. Groot VP, Rezaee N, Wu W, Cameron JL, Fishman EK, Hruban RH, et al. Patterns, Timing, and Predictors of Recurrence Following Pancreatectomy for Pancreatic Ductal Adenocarcinoma. Ann Surg. 2017.
8. Paez D, Labonte MJ, Bohanes P, Zhang W, Benhanim L, Ning Y, et al. Cancer dormancy: a model of early dissemination and late cancer recurrence. Clin Cancer Res. 2012;18:645–53. [PubMed: 22156560]
9. Racanelli V, Rehermann B. The liver as an immunological organ. Hepatology. 2006;43:S54–62. [PubMed: 16447271]
10. Heymann F, Tacke F. Immunology in the liver--from homeostasis to disease. Nat Rev Gastroenterol Hepatol. 2016;13:88–110. [PubMed: 26758786]
11. Allavena P, Sica A, Solinas G, Porta C, Mantovani A The inflammatory microenvironment in tumor progression: the role of tumor-associated macrophages. Crit Rev Oncol/Hematol. 2008;66:1–9.
12. Kurahara H, Shinchi H, Mataki Y, Maemura K, Noma H, Kubo F, et al. Significance of M2-polarized tumor-associated macrophage in pancreatic cancer. J Surg Res. 2011;167:e211–9. [PubMed: 19765725]
13. Heuff G, Oldenburg HS, Boutkan H, Visser JJ, Beelen RH, Van Rooijen N, et al. Enhanced tumour growth in the rat liver after selective elimination of Kupffer cells. Cancer Immunol Immunother. 1993;37:125–30. [PubMed: 8319242]
14. Gangopadhyay A, Lazure DA, Thomas P. Adhesion of colorectal carcinoma cells to the endothelium is mediated by cytokines from CEA stimulated Kupffer cells. Clin Exp Metastasis. 1998;16:703–12. [PubMed: 10211983]
15. Timmers M, Vekemans K, Vermijlen D, Asosingh K, Kuppen P, Bouwens L, et al. Interactions between rat colon carcinoma cells and Kupffer cells during the onset of hepatic metastasis. Int J Cancer. 2004;112:793–802. [PubMed: 15386374]
16. Nielsen SR, Quaranta V, Linford A, Emeagi P, Rainer C, Santos A, et al. Macrophage-secreted granulin supports pancreatic cancer metastasis by inducing liver fibrosis. Nat Cell Biol. 2016;18:549–60. [PubMed: 27088855]
17. Qian BZ, Zhang H, Li J, He T, Yeo EJ, Soong DY, et al. FLT1 signaling in metastasis-associated macrophages activates an inflammatory signature that promotes breast cancer metastasis. J Exp Med. 2015;212:1433–48. [PubMed: 26261265]
18. Gul N, Babes L, Siegmund K, Korthouwer R, Bogels M, Braster R, et al. Macrophages eliminate circulating tumor cells after monoclonal antibody therapy. J Clin Invest. 2014;124:812–23. [PubMed: 24430180]
19. Cioffi M, Trabulo S, Hidalgo M, Costello E, Greenhalf W, Erkan M, et al. Inhibition of CD47 Effectively Targets Pancreatic Cancer Stem Cells via Dual Mechanisms. Clin Cancer Res. 2015;21:2325–37. [PubMed: 25717063]
20. Jaiswal S, Jamieson CH, Pang WW, Park CY, Chao MP, Majeti R, et al. CD47 is upregulated on circulating hematopoietic stem cells and leukemia cells to avoid phagocytosis. Cell. 2009;138:271–85. [PubMed: 19632178]
21. Sick E, Jeanne A, Schneider C, Dedieu S, Takeda K, Martiny L. CD47 update: a multifaceted actor in the tumour microenvironment of potential therapeutic interest. Br J Pharmacol. 2012;167:1415–30. [PubMed: 22774848]
22. Willingham SB, Volkmer JP, Gentles AJ, Sahoo D, Dalerba P, Mitra SS, et al. The CD47-signal regulatory protein alpha (SIRPa) interaction is a therapeutic target for human solid tumors. Proc Natl Acad Sci U S A. 2012;109:6662–7. [PubMed: 22451913]

23. Tseng D, Volkmer JP, Willingham SB, Contreras-Trujillo H, Fathman JW, Fernhoff NB, et al. Anti-CD47 antibody-mediated phagocytosis of cancer by macrophages primes an effective antitumor T-cell response. Proc Natl Acad Sci U S A. 2013;110:11103–8. [PubMed: 23690610]
24. Walters DM, Stokes JB, Adair SJ, Stelow EB, Borgman CA, Lowrey BT, et al. Clinical, molecular and genetic validation of a murine orthotopic xenograft model of pancreatic adenocarcinoma using fresh human specimens. PLoS One. 2013;8:e77065. [PubMed: 24204737]
25. Stokes JB, Adair SJ, Slack-Davis JK, Walters DM, Tilghman RW, Hershey ED, et al. Inhibition of focal adhesion kinase by PF-562,271 inhibits the growth and metastasis of pancreatic cancer concomitant with altering the tumor microenvironment. Mol Cancer Ther. 2011;10:2135–45. [PubMed: 21903606]
26. Newhook TE, Lindberg JM, Adair SJ, Kim AJ, Stelow EB, Rahma OE, et al. Adjuvant Trametinib Delays the Outgrowth of Occult Pancreatic Cancer in a Mouse Model of Patient-Derived Liver Metastasis. Annals of Surgical Oncology. 2016;23:1993–2000. [PubMed: 26847682]
27. Van Rooijen N, Sanders A. Liposome mediated depletion of macrophages: mechanism of action, preparation of liposomes and applications. J Immunol Methods. 1994;174:83–93. [PubMed: 8083541]
28. Han CZ, Juncadella IJ, Kinchen JM, Buckley MW, Klibanov AL, Dryden K, et al. Macrophages redirect phagocytosis by non-professional phagocytes and influence inflammation. Nature. 2016;539:570–4. [PubMed: 27820945]
29. Tsai RK, Discher DE. Inhibition of “self” engulfment through deactivation of myosin-II at the phagocytic synapse between human cells. J Cell Biol. 2008;180:989–1003. [PubMed: 18332220]
30. Aguirre-Ghiso JA, Bragado P, Sosa MS. Metastasis awakening: targeting dormant cancer. Nat Med. 2013;19:276–7. [PubMed: 23467238]
31. Griesmann H, Drexel C, Milosevic N, Sipos B, Rosendahl J, Gress TM, et al. Pharmacological macrophage inhibition decreases metastasis formation in a genetic model of pancreatic cancer. Gut. 2017;66:1278–85. [PubMed: 27013602]
32. Xiao Z, Chung H, Banan B, Manning PT, Ott KC, Lin S, et al. Antibody mediated therapy targeting CD47 inhibits tumor progression of hepatocellular carcinoma. Cancer Lett. 2015;360:302–9. [PubMed: 25721088]
33. Ravichandran KS. Find-me and eat-me signals in apoptotic cell clearance: progress and conundrums. J Exp Med. 2010;207:1807–17. [PubMed: 20805564]
34. Krampitz GW, George BM, Willingham SB, Volkmer JP, Weiskopf K, Jahchan N, et al. Identification of tumorigenic cells and therapeutic targets in pancreatic neuroendocrine tumors. Proc Natl Acad Sci U S A. 2016;113:4464–9. [PubMed: 27035983]
35. Sanchez-Garcia I The crossroads of oncogenesis and metastasis. N Engl J Med. 2009;360:297–9. [PubMed: 19144947]
36. Klein CA. Parallel progression of primary tumours and metastases. Nature reviews Cancer. 2009;9:302–12. [PubMed: 19308069]
37. Haeno H, Gonen M, Davis MB, Herman JM, Iacobuzio-Donahue CA, Michor F. Computational modeling of pancreatic cancer reveals kinetics of metastasis suggesting optimum treatment strategies. Cell. 2012;148:362–75. [PubMed: 22265421]
38. McDonald OG, Li X, Saunders T, Tryggvadottir R, Mentch SJ, Warmoes MO, et al. Epigenomic reprogramming during pancreatic cancer progression links anabolic glucose metabolism to distant metastasis. Nat Genet. 2017;49:367–76. [PubMed: 28092686]
39. Rhim AD, Mirek ET, Aiello NM, Maitra A, Bailey JM, McAllister F, et al. EMT and dissemination precede pancreatic tumor formation. Cell. 2012;148:349–61. [PubMed: 22265420]
40. Turcotte S, Jarnagin WR. Liver & Portal Venous System In: Doherty GM, editor. CURRENT Diagnosis & Treatment: Surgery 14 ed New York: McGraw-Hill; 2014.
41. Malladi S, Macalinao DG, Jin X, He L, Basnet H, Zou Y, et al. Metastatic Latency and Immune Evasion through Autocrine Inhibition of WNT. Cell. 2016;165:45–60. [PubMed: 27015306]
42. Sosale NG, Spinler KR, Alvey C, Discher DE. Macrophage engulfment of a cell or nanoparticle is regulated by unavoidable opsonization, a species-specific ‘Marker of Self’ CD47, and target physical properties. Curr Opin Immunol. 2015;35:107–12. [PubMed: 26172292]

Translational Relevance:

Patients with early-stage pancreatic cancer who undergo surgical resection and receive adjuvant chemotherapy have a median survival of two years, mostly due to the presence and eventual progression of undetectable micrometastatic disease in the liver. In a preclinical murine model, we show that liver macrophages significantly slow the progression of pancreatic cancer micrometastases. The suppressive effect of macrophages was enhanced by blocking CD47 on pancreatic cancer cells, leading to decreased metastatic burden and prolonged survival. This work supports a clinical trial of CD47 blockade as an adjuvant immunotherapy for pancreatic cancer.

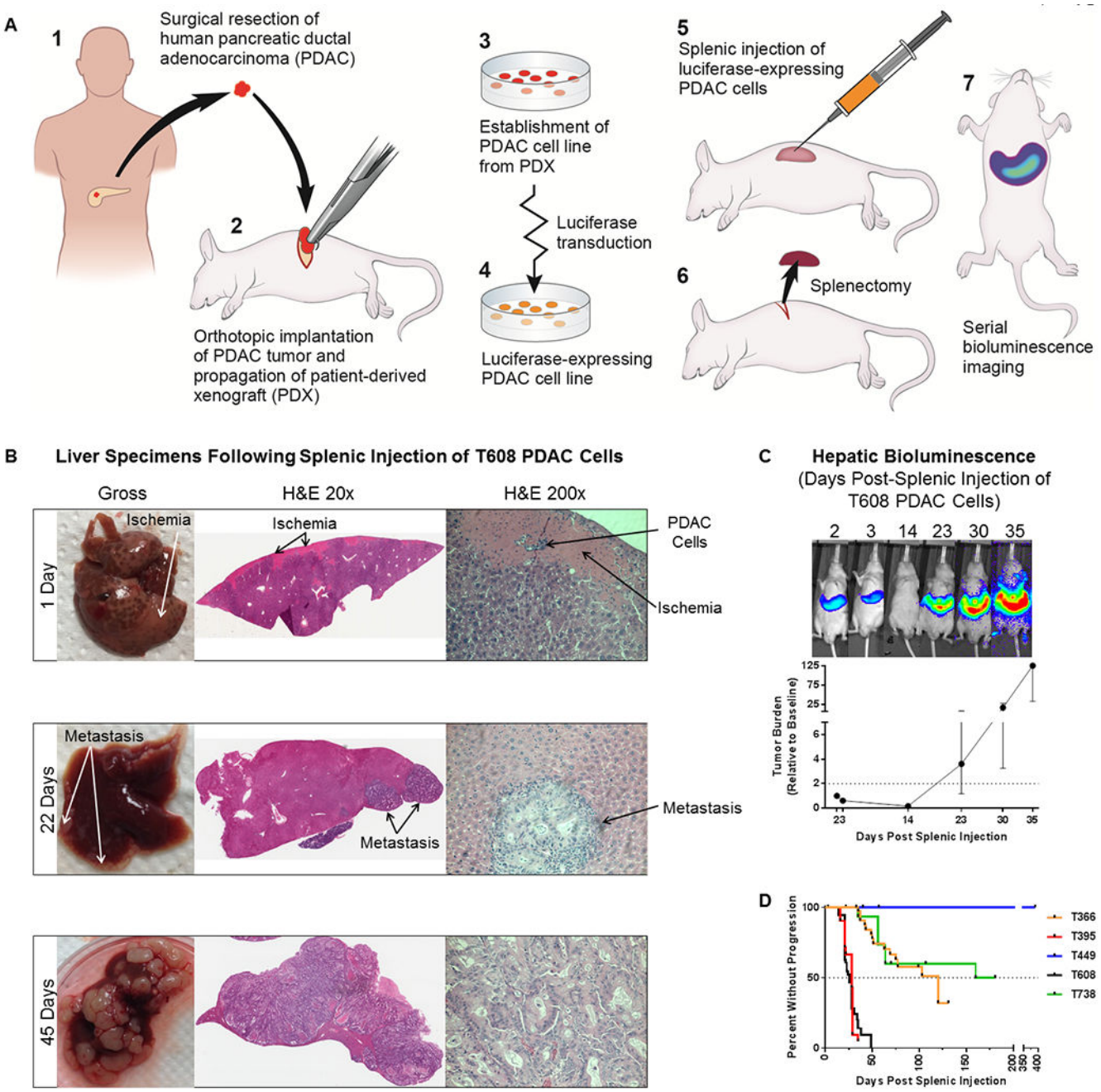

Fig 1. *In vivo* model of hepatic micrometastatic pancreatic ductal adenocarcinoma (PDAC).

A) Schematic of PDAC cell line establishment and the *in vivo* model. B) Gross necropsy specimens and H&E staining of livers harvested from mice at 1 day, 22 days, and 45 days after splenic injection of patient-derived PDAC (T608) cells. C) Hepatic tumor burden is tracked with serial *in vivo* bioluminescence imagining. A representative mouse at different time points following splenic injection of PDAC (T608) cells (top) and a growth curve of hepatic tumor burden relative to 48 hours post-splenic injection (n = 11). Data are expressed as median ± interquartile range. The dotted line represents a relative hepatic tumor burden of 2.0, defined as disease progression. D) Kaplan-Meier curves of time-to-progression for five

patient-derived PDAC cell lines (T366: n = 38, T395: n = 21, T449: n = 14, T608: n = 101, T738: n = 15).

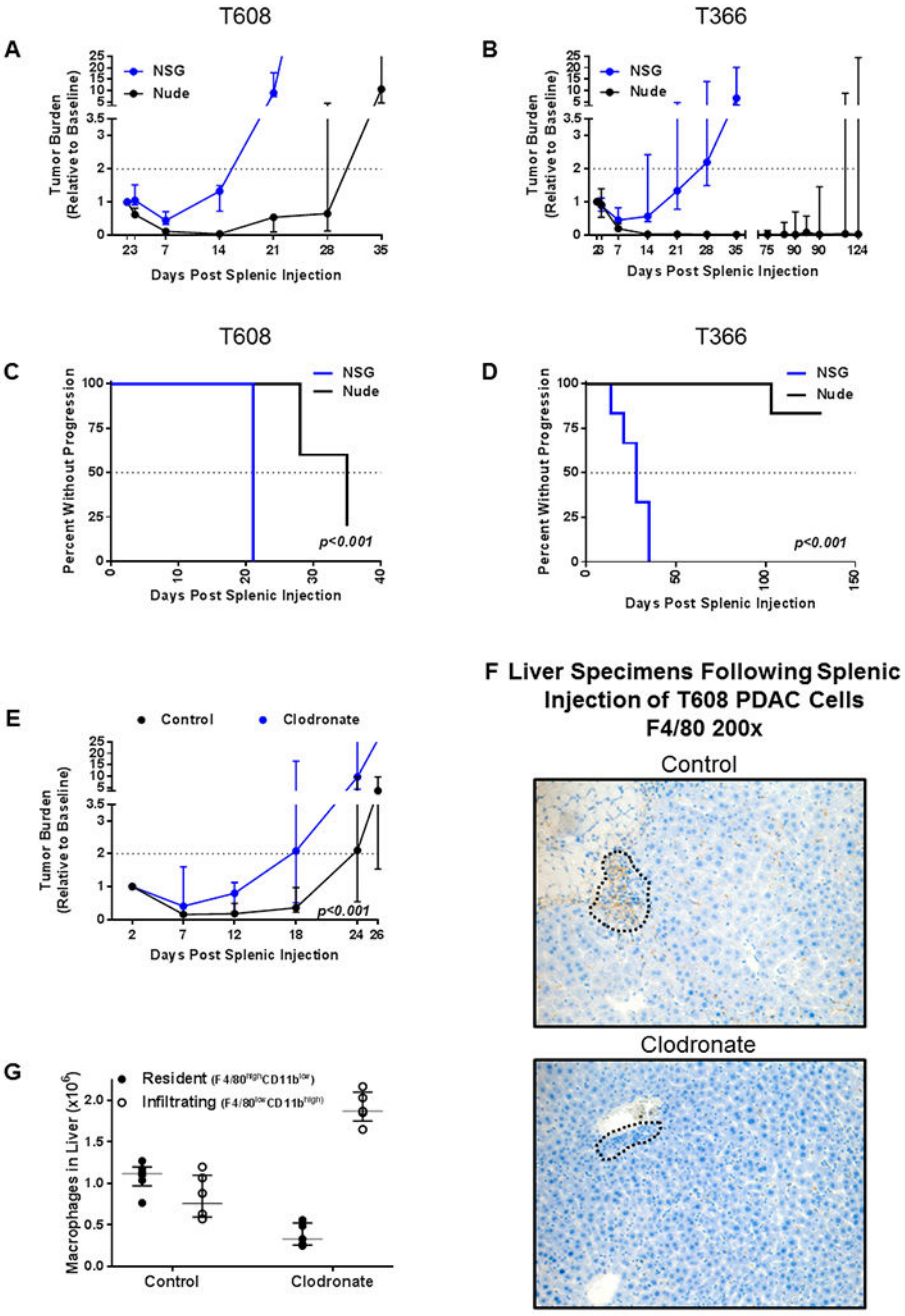

Fig 2. The role of the macrophages in suppressing the progression of pancreatic ductal adenocarcinoma (PDAC) micrometastases.

Growth curves of hepatic tumor burden in athymic nude mice (Nude, black) vs NOD *scid* gamma (NSG, blue) following splenic injection of A) T608 (n = 5-7 per group) and B) T366 (n = 5-6 per group) patient-derived PDAC cells. Data are expressed as median ± interquartile range. Mann-Whitney test was used to compare tumor burdens. Kaplan-Meier curves showing that time-to-progression (TTP) was significantly accelerated in NSG mice (blue) vs nude mice (black) in both C) T608 and D) T366. Log-rank test was used to compare TTP between groups. E) Growth curves of hepatic tumor burden in nude mice which underwent

ablation of resident liver macrophages with intraperitoneal clodronate (blue, n = 5) vs untreated nude mice (black, n = 10) following splenic injection of T608 patient-derived PDAC cells. Two-way ANOVA with repeated measures was used to compare the two groups. F) Representative anti-F4/80 IHC (200x magnification) three days after splenic injection of T608 patient-derived PDAC cells reveals an abundance of macrophages (brown) in the livers of untreated nude mice (top) and no macrophages in the livers of nude mice treated with clodronate (bottom). Areas containing dense collections of PDAC cells are outlined. G) Flow cytometric analysis of liver digests two to three days after splenic injection of T608 patient-derived PDAC cells demonstrating the selective ablation of resident liver macrophages ($F4/80^{high}CD11b^{low}$, closed circles) and preserved infiltration of circulating monocytes ($F4/80^{low}CD11b^{high}$, open circles) in untreated (n = 6) and clodronate-treated (n = 5) nude mice. Data are expressed as median ± interquartile range.

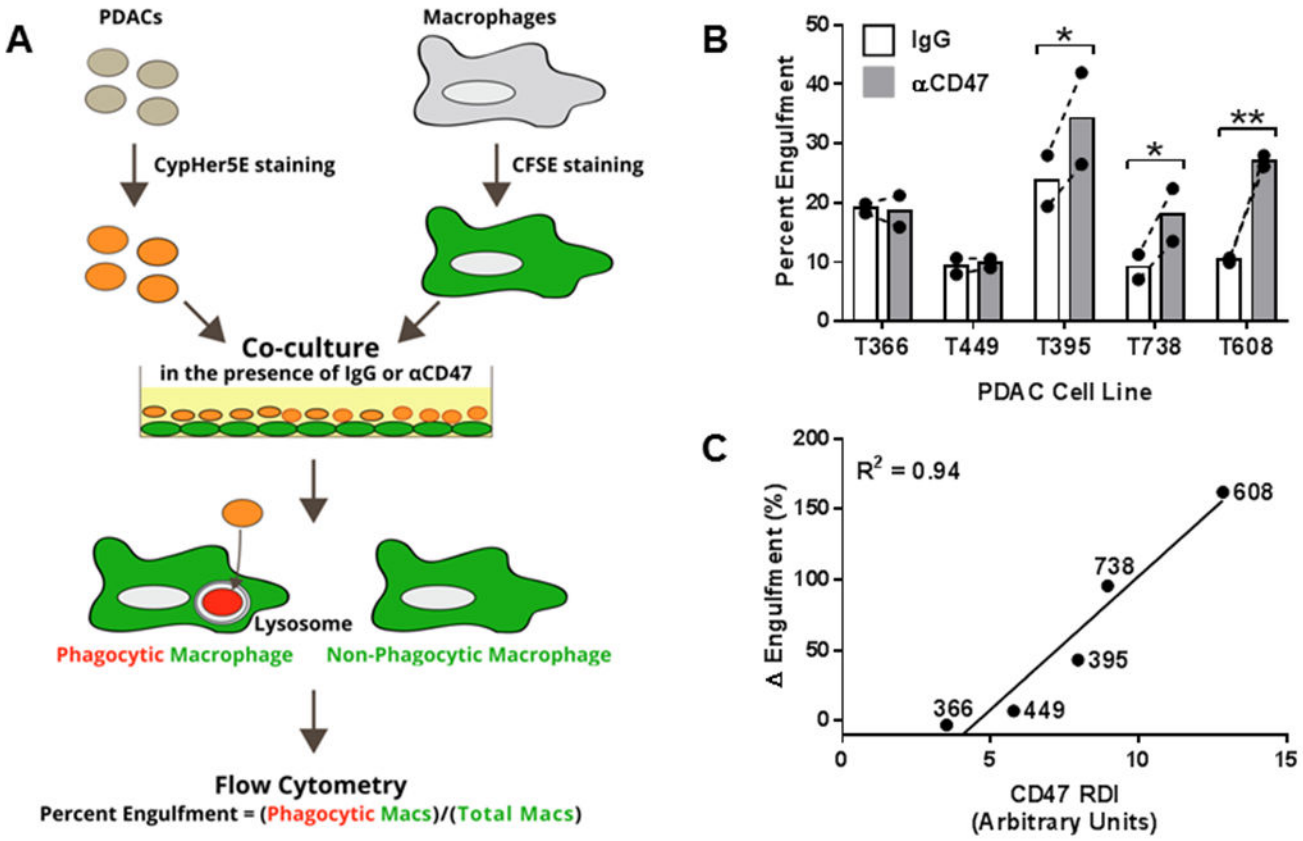

Fig 3. Enhancement of *in vitro* engulfment of patient-derived pancreatic ductal adenocarcinoma (PDAC) cells with CD47 blockade.

A) Schematic of the *in vitro* engulfment assay protocol. B) Percent engulfment of five patient-derived PDAC cell lines in the presence of purified IgG from mouse serum (IgG) or a blocking anti-CD47 antibody (αCD47). Bars represent mean percent engulfment under each condition, closed circles represent individual experiments, and the dashed lines connect data within an individual experiment. Experiments were performed twice, each with three technical replicates. Paired t-test was used to compare engulfment percentages under different treatments. Significance is denoted as * $p<0.05$ and ** $p<0.01$. C) Pearson's correlation between CD47 receptor density index (RDI) and Δ Engulfment (Percent $\text{Engulfment}_{\alpha\text{CD47-Treated}}$/Percent $\text{Engulfment}_{\text{Mouse IgG-Treated}}$).

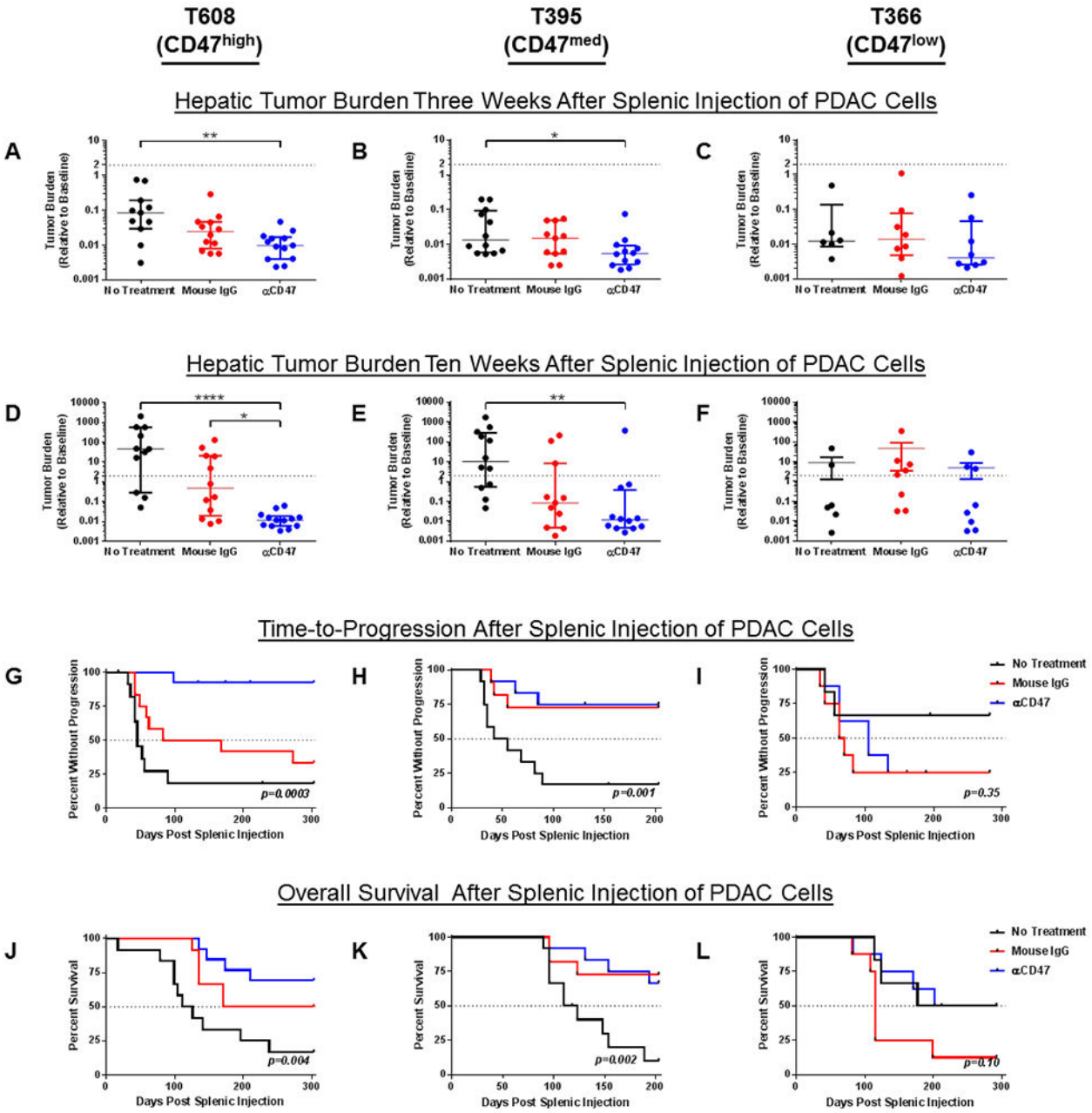

Fig 4. Effect of CD47 blockade on micrometastatic pancreatic ductal adenocarcinoma (PDAC) tumor burden, time-to-progression, and survival.

The effects on tumor burden of daily therapy with a blocking anti-CD47 antibody (αCD47, blue), purified IgG from mouse serum (Mouse IgG, red), or no treatment (black) in A) T608 at 24 days post-splenic injection (n = 11-13 per group), B) T395 at 22 days post splenic injection (n = 11-12 per group), and C) T366 at 24 days post splenic injection (n = 6-9 per group). Dot plots of tumor burden in the three treatment groups 3-7 weeks after the cessation of therapy in D) T608 at 69 days, E) T395 and 68 days, and F) 69 days. The dotted line represents a relative hepatic tumor burden of 2.0, defined as disease progression. Data are

expressed as median ± interquartile range. Kruskal-Wallis test with Dunn's test for multiple comparisons was used to compare tumor burdens. Significance is denoted as * $p<0.05$, ** $p<0.01$, *** $p<0.001$, **** $p<0.0001$. G-I) Kaplan-Meier curves of time-to-progression (TTP) for mice bearing the indicated tumors under the three treatment conditions. J-L) Kaplan-Meier curves of overall survival (OS) for mice bearing the indicated tumors under the three treatment conditions. TTP and OS among treatment groups were compared using log-rank test.

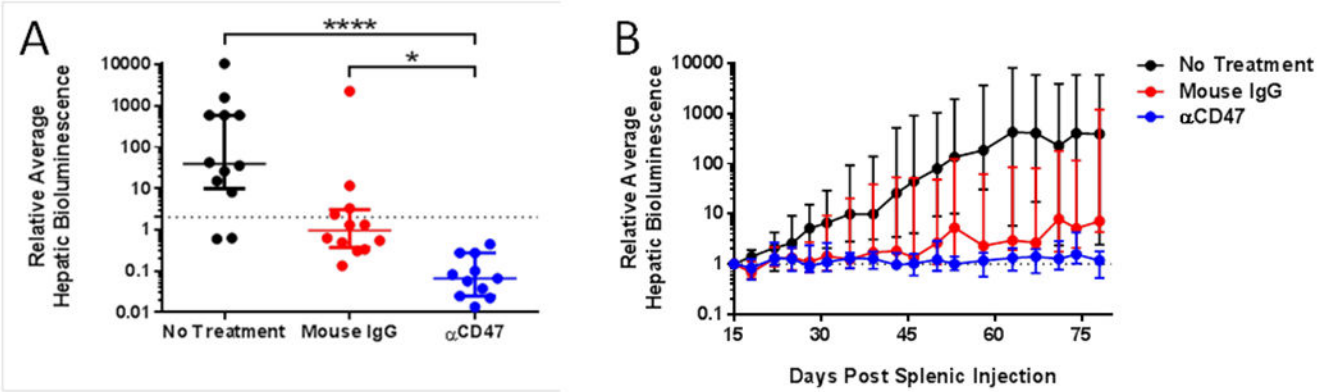

Fig 5. Effect of short-course or delayed-course CD47 blockade on micrometastatic pancreatic ductal adenocarcinoma (PDAC) tumor burden.

A) Evaluation of short-course αCD47 antibody treatment. Dot plots of tumor burden at 58 days post-splenic injection following daily therapy from days 2-22 with a blocking anti-CD47 antibody (αCD47, blue), purified IgG from mouse serum (Mouse IgG, red), or no treatment (black) in mice bearing T608 (n = 11-12 per group). The dotted line represents a relative hepatic tumor burden of 2.0, defined as disease progression. Data are expressed as median ± interquartile range. Kruskal-Wallis test with Dunn's test for multiple comparisons was used to compare tumor burdens. Significance is denoted as * $p<0.05$, ** $p<0.01$, *** $p<0.001$, **** $p<0.0001$. B) Effect of delayed-course αCD47 antibody treatment. Growth curves of hepatic tumor burden relative to 15 days post-splenic injection in mice bearing T608 which received daily therapy with a blocking anti-CD47 antibody (αCD47, blue), purified IgG from mouse serum (Mouse IgG, red), or no treatment (black) from days 15-35 (n = 11-12 per group). Tumor burden at 78 days was significantly lower in mice treated with αCD47 (no treatment vs Mouse IgG: $p=0.99$, no treatment vs αCD47: $p=0.004$, Mouse IgG vs αCD47: $p=0.006$). Data are expressed as median ± interquartile range. The dotted line represents a relative hepatic tumor burden of 1.0. Kruskal-Wallis test with Dunn's test for multiple comparisons was used to compare tumor burdens.

Table 1.

CD47 surface expression of patient-derived pancreatic ductal adenocarcinoma (PDAC) cell lines.

Flow cytometric analysis of CD47 expression of five PDAC cell lines. These data represent three independent experiments and are expressed as mean ± standard error. MFI, median fluorescence intensity; FSC, forward scatter.

	T366	T449	T395	T738	T608
CD47 MFI (Arbitrary Units)	182±35	285±64	319±168	315±27	547±118
FSC ($\times 10^3$ Arbitrary Units)	71.7±4.7	71.8±5.4	64.0±3.4	60.5±3.3	66.3±2.1
CD47 Surface Receptor Density Index (Arbitrary Units)	3.5±0.6	5.8±1.7	8.0±2.1	9.0±1.9	12.9±3.6